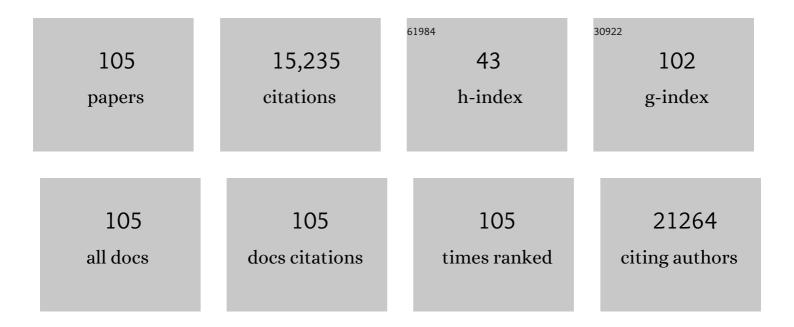
List of Publications by Year in descending order

Source: https://exaly.com/author-pdf/5250345/publications.pdf Version: 2024-02-01



#	Article	IF	CITATIONS
1	Second-harmonic generation in atomically thin <mml:math xmlns:mml="http://www.w3.org/1998/Math/MathML"><mml:mn>1</mml:mn><mml:mi>T</mml:mi><mml:mte and its possible origin from charge density wave transitions. Physical Review B, 2022, 105, .</mml:mte </mml:math 	xt> ấ:ỉ₂ /mn	nl:natext> <nu< td=""></nu<>
2	Deep Elastic Strain Engineering of 2D Materials and Their Twisted Bilayers. ACS Applied Materials & Interfaces, 2022, 14, 8655-8663.	8.0	16
3	Tuning the morphology of 2D transition metal chalcogenides via oxidizing conditions. Journal of Physics Condensed Matter, 2022, 34, 195001.	1.8	3
4	Compression behaviors of the bio-inspired hierarchical lattice structure with improved mechanical properties and energy absorption capacity. Journal of Materials Research and Technology, 2022, 17, 2755-2771.	5.8	20
5	Dual-Mode Flexible Capacitive Sensor for Proximity-Tactile Interface and Wireless Perception. IEEE Sensors Journal, 2022, 22, 10446-10453.	4.7	14
6	Monolayer MoS2-Based Flexible and Highly Sensitive Pressure Sensor with Wide Sensing Range. Micromachines, 2022, 13, 660.	2.9	8
7	Flexible Pressure Sensor With Wide Linear Sensing Range for Human–Machine Interaction. IEEE Transactions on Electron Devices, 2022, 69, 3901-3907.	3.0	7
8	Boosting the performance of single-atom catalysts via external electric field polarization. Nature Communications, 2022, 13, .	12.8	52
9	Flexible Gas-Permeable and Resilient Bowtie Antenna for Tensile Strain and Temperature Sensing. IEEE Internet of Things Journal, 2022, 9, 23215-23223.	8.7	2
10	A Bayesian inverse approach to measure the anisotropic plasticity properties of materials using spherical indentation experiment. Measurement: Journal of the International Measurement Confederation, 2021, 171, 108812.	5.0	6
11	Architectured graphene and its composites: Manufacturing and structural applications. Composites Part A: Applied Science and Manufacturing, 2021, 140, 106177.	7.6	22
12	Superconductivity in two-dimensional ÎMo3C2 films. Science China Materials, 2021, 64, 664-672.	6.3	3
13	Enhancing stability by tuning element ratio in 2D transition metal chalcogenides. Nano Research, 2021, 14, 1704-1710.	10.4	10
14	Chemical vapour deposition. Nature Reviews Methods Primers, 2021, 1, .	21.2	244
15	Experimental nanomechanics of 2D materials for strain engineering. Applied Nanoscience (Switzerland), 2021, 11, 1075-1091.	3.1	20
16	Three-Dimensional Stretchable Microelectronics by Projection Microstereolithography (PμSL). ACS Applied Materials & Interfaces, 2021, 13, 8901-8908.	8.0	19
17	Stereolithography (SLA) 3D printing of carbon fiber-graphene oxide (CF-GO) reinforced polymer lattices. Nanotechnology, 2021, 32, 235702.	2.6	30
18	Magnetically induced micropillar arrays for an ultrasensitive flexible sensor with a wireless recharging system. Science China Materials, 2021, 64, 1977-1988.	6.3	13

#	Article	IF	CITATIONS
19	Highly Sensitive Pseudocapacitive Iontronic Pressure Sensor with Broad Sensing Range. Nano-Micro Letters, 2021, 13, 140.	27.0	69
20	3D printing of dual phase-strengthened microlattices for lightweight micro aerial vehicles. Materials and Design, 2021, 206, 109767.	7.0	35
21	Wearable, self-cleaning, wireless integrated tactile sensory system with superior sensitivity. Sensors and Actuators A: Physical, 2021, 331, 113027.	4.1	5
22	Stretchable and anti-impact iontronic pressure sensor with an ultrabroad linear range for biophysical monitoring and deep learning-aided knee rehabilitation. Microsystems and Nanoengineering, 2021, 7, 92.	7.0	30
23	A Molecular Dynamics Simulation Study: The Inkjet Printing of Graphene Inks on Polyimide Substrates. Frontiers in Materials, 2021, 8, .	2.4	0
24	Nano electromechanical approach for flexible piezoresistive sensor. Applied Materials Today, 2020, 18, 100475.	4.3	16
25	Proton-assisted growth of ultra-flat graphene films. Nature, 2020, 577, 204-208.	27.8	111
26	Thermal Effect and Rayleigh Instability of Ultrathin 4H Hexagonal Gold Nanoribbons. Matter, 2020, 2, 658-665.	10.0	30
27	Tuning the Electronic Structure of an α-Antimonene Monolayer through Interface Engineering. Nano Letters, 2020, 20, 8408-8414.	9.1	33
28	Large Elastic Deformation and Defect Tolerance of Hexagonal Boron Nitride Monolayers. Cell Reports Physical Science, 2020, 1, 100172.	5.6	23
29	In situ mechanical characterization of silver nanowire/graphene hybrids films for flexible electronics. International Journal of Smart and Nano Materials, 2020, 11, 265-276.	4.2	10
30	Flexible Waterproof Piezoresistive Pressure Sensors with Wide Linear Working Range Based on Conductive Fabrics. Nano-Micro Letters, 2020, 12, 159.	27.0	53
31	Anisotropic scattering continuum induced by crystal symmetry reduction in atomically thin <mml:math xmlns:mml="http://www.w3.org/1998/Math/MathML"><mml:mi>î±</mml:mi><mml:mo>–</mml:mo><mml:m /><mml:mn>3</mml:mn>. Physical Review B, 2020, 101, .</mml:m </mml:math 	ii>RửĈl <td>ıml:mi><mn< td=""></mn<></td>	ıml : mi> <mn< td=""></mn<>
32	Elastic straining of free-standing monolayer graphene. Nature Communications, 2020, 11, 284.	12.8	194
33	3D printing of titanium-coated gradient composite lattices for lightweight mandibular prosthesis. Composites Part B: Engineering, 2020, 193, 108057.	12.0	67
34	Cold welding assisted self-healing of fractured ultrathin Au nanowires. Nano Express, 2020, 1, 020014.	2.4	6
35	Biomimetic and Radially Symmetric Graphene Aerogel for Flexible Electronics. Advanced Electronic Materials, 2019, 5, 1900353.	5.1	14
36	Reliability of tensile fracture strength of Co-based metallic glass microwires by Weibull statistics. Materials Research Express, 2019, 6, 106565.	1.6	3

#	Article	IF	CITATIONS
37	<i>In situ</i> tensile fracturing of multilayer graphene nanosheets for their in-plane mechanical properties. Nanotechnology, 2019, 30, 475708.	2.6	17
38	3D printed micro-mechanical device (MMD) for in situ tensile testing of micro/nanowires. Extreme Mechanics Letters, 2019, 33, 100575.	4.1	12
39	Highly stretchable graphene nanoribbon springs by programmable nanowire lithography. Npj 2D Materials and Applications, 2019, 3, .	7.9	20
40	Molecular dynamics study on explosive boiling of ultra-thin liquid over solid substrate: considering interface wettability of Argon/MoS ₂ . Molecular Simulation, 2019, 45, 996-1003.	2.0	3
41	Cellular Carbon-Film-Based Flexible Sensor and Waterproof Supercapacitors. ACS Applied Materials & Interfaces, 2019, 11, 26288-26297.	8.0	28
42	Stereolithographic 3D Printing-Based Hierarchically Cellular Lattices for High-Performance Quasi-Solid Supercapacitor. Nano-Micro Letters, 2019, 11, 46.	27.0	62
43	Novel 2D metamaterials with negative Poisson's ratio and negative thermal expansion. Extreme Mechanics Letters, 2019, 30, 100498.	4.1	80
44	Turning ZrTe5 into a semiconductor through atom intercalation. Science China: Physics, Mechanics and Astronomy, 2019, 62, 1.	5.1	5
45	Growth of environmentally stable transition metal selenide films. Nature Materials, 2019, 18, 602-607.	27.5	116
46	Mechanical Metamaterials and Their Engineering Applications. Advanced Engineering Materials, 2019, 21, 1800864.	3.5	493
47	Molecular Dynamics Simulation of Self-assembly and Electroporation of Lipid Bilayer Membrane in Martini Force Field. , 2019, , .		1
48	Atomic Study on Tension Behaviors of Sub-10 nm NanoPolycrystalline Cu–Ta Alloy. Materials, 2019, 12, 3913.	2.9	8
49	NiO-bridged MnCo-hydroxides for flexible high-performance fiber-shaped energy storage device. Applied Surface Science, 2019, 475, 1058-1064.	6.1	48
50	Van der Waals Heteroepitaxial Growth of Monolayer Sb in a Puckered Honeycomb Structure. Advanced Materials, 2019, 31, e1806130.	21.0	75
51	Highâ€Frequency Flexible Graphene Fieldâ€Effect Transistors with Short Gate Length of 50 nm and Record Extrinsic Cutâ€Off Frequency. Physica Status Solidi - Rapid Research Letters, 2018, 12, 1700435.	2.4	5
52	Enhancing the Strength of Graphene by a Denser Grain Boundary. ACS Nano, 2018, 12, 4529-4535.	14.6	39
53	Mechanical Enhancement of Core-Shell Microlattices through High-Entropy Alloy Coating. Scientific Reports, 2018, 8, 5442.	3.3	30
54	Mechanically stable ternary heterogeneous electrodes for energy storage and conversion. Nanoscale, 2018, 10, 2613-2622.	5.6	28

#	Article	IF	CITATIONS
55	Size-dependent fracture behavior of silver nanowires. Nanotechnology, 2018, 29, 295703.	2.6	18
56	Dendrite-free Li metal anode by lowering deposition interface energy with Cu99Zn alloy coating. Energy Storage Materials, 2018, 14, 143-148.	18.0	99
57	Highâ€Entropy Alloy (HEA)â€Coated Nanolattice Structures and Their Mechanical Properties. Advanced Engineering Materials, 2018, 20, 1700625.	3.5	56
58	Preparation of Ultra-Smooth Cu Surface for High-Quality Graphene Synthesis. Nanoscale Research Letters, 2018, 13, 340.	5.7	8
59	Ultra-Flexible and Large-Area Textile-Based Triboelectric Nanogenerators with a Sandpaper-Induced Surface Microstructure. Materials, 2018, 11, 2120.	2.9	24
60	Direct quantification of mechanical responses of TiSiN/Ag multilayer coatings through uniaxial compression of micropillars. Vacuum, 2018, 156, 310-316.	3.5	25
61	Graphene-Bridged Multifunctional Flexible Fiber Supercapacitor with High Energy Density. ACS Applied Materials & Interfaces, 2018, 10, 28597-28607.	8.0	73
62	Metal-coated hybrid meso-lattice composites and their mechanical characterizations. Composite Structures, 2018, 203, 750-763.	5.8	40
63	Mechanical Properties of Nanostructured CoCrFeNiMn High-Entropy Alloy (HEA) Coating. Frontiers in Materials, 2018, 5, .	2.4	43
64	Flexible Fiber-Shaped Supercapacitor Based on Nickel–Cobalt Double Hydroxide and Pen Ink Electrodes on Metallized Carbon Fiber. ACS Applied Materials & Interfaces, 2017, 9, 5409-5418.	8.0	147
65	In situ nanomechanical characterization of multi-layer MoS ₂ membranes: from intraplanar to interplanar fracture. Nanoscale, 2017, 9, 9119-9128.	5.6	39
66	Rationally designed nickel oxide ravines@iron cobalt-hydroxides with largely enhanced capacitive performance for asymmetric supercapacitors. Journal of Materials Chemistry A, 2017, 5, 16944-16952.	10.3	37
67	Nanocrystalline high-entropy alloy (CoCrFeNiAl0.3) thin-film coating by magnetron sputtering. Thin Solid Films, 2017, 638, 383-388.	1.8	128
68	Microstructure, Mechanical and Corrosion Behaviors of CoCrFeNiAl0.3 High Entropy Alloy (HEA) Films. Coatings, 2017, 7, 156.	2.6	47
69	Self-assembly of hierarchical 3D starfish-like Co3O4 nanowire bundles on nickel foam for high-performance supercapacitor. Journal of Nanoparticle Research, 2016, 18, 1.	1.9	25
70	Heteroepitaxial growth of wafer scale highly oriented graphene using inductively coupled plasma chemical vapor deposition. 2D Materials, 2016, 3, 021001.	4.4	12
71	Elemental superdoping of graphene and carbon nanotubes. Nature Communications, 2016, 7, 10921.	12.8	238
72	Investigation of lattice distortion of Co3O4 nanoparticles prepared by a carbon-assisted method. Microelectronic Engineering, 2016, 159, 17-20.	2.4	9

#	Article	IF	CITATIONS
73	Facile synthesis of core–shell structured PANI-Co3O4 nanocomposites with superior electrochemical performance in supercapacitors. Applied Surface Science, 2016, 361, 57-62.	6.1	106
74	Chemical Vapor Deposition of Large‣ized Hexagonal WSe ₂ Crystals on Dielectric Substrates. Advanced Materials, 2015, 27, 6722-6727.	21.0	152
75	Largeâ€Area, Periodic, Hexagonal Wrinkles on Nanocrystalline Graphitic Film. Advanced Functional Materials, 2015, 25, 5492-5503.	14.9	16
76	A Novel Arch-Shape Nanogenerator Based on Piezoelectric and Triboelectric Mechanism for Mechanical Energy Harvesting. Nanomaterials, 2015, 5, 36-46.	4.1	49
77	Synthesis and Microwave Absorption Properties of Core-Shell Structured Co ₃ O ₄ -PANI Nanocomposites. Journal of Nanomaterials, 2015, 2015, 1-8.	2.7	32
78	A Green and Facile Synthesis of Carbon-Incorporated Co ₃ O ₄ Nanoparticles and Their Photocatalytic Activity for Hydrogen Evolution. Journal of Nanomaterials, 2015, 2015, 1-7.	2.7	15
79	Synthesis of octahedral Co ₃ O ₄ via carbonâ€assisted method. Micro and Nano Letters, 2015, 10, 85-87.	1.3	4
80	Photocatalytic Property of Fe ₃ O ₄ /SiO ₂ /TiO ₂ Core-Shell Nanoparticle with Different Functional Layer Thicknesses. Journal of Nanomaterials, 2014, 2014, 1-7.	2.7	9
81	Preparation Method of Co ₃ O ₄ Nanoparticles Using Degreasing Cotton and Their Electrochemical Performances in Supercapacitors. Journal of Nanomaterials, 2014, 2014, 1-9.	2.7	13
82	Face-to-face transfer of wafer-scale graphene films. Nature, 2014, 505, 190-194.	27.8	386
83	Giant enhancement in vertical conductivity of stacked CVD graphene sheets by self-assembled molecular layers. Nature Communications, 2014, 5, 5461.	12.8	83
84	Adsorption of Methyl Orange on Magnetically Separable Mesoporous Titania Nanocomposite. Chinese Journal of Chemical Engineering, 2014, 22, 1168-1173.	3.5	14
85	Investigation of TiO <inf>2</inf> -SiO <inf>2</inf> -Fe <inf>3</inf> O <inf>4</inf> core-shell nanoparticle properties with different functional layer thickness. , 2013, , .		0
86	Synthesis of superparamagnetic iron oxide nanoparticles in carbon reduction method. Micro and Nano Letters, 2013, 8, 598-601.	1.3	13
87	Wall-number selective growth of vertically aligned carbon nanotubes from FePt catalysts: a comparative study with Fe catalysts. Journal of Materials Chemistry, 2012, 22, 14149.	6.7	9
88	Repeated growth and bubbling transfer of graphene with millimetre-size single-crystal grains using platinum. Nature Communications, 2012, 3, 699.	12.8	985
89	Three-dimensional flexible and conductive interconnected graphene networks grown by chemical vapour deposition. Nature Materials, 2011, 10, 424-428.	27.5	3,493
90	Additiveâ€Free Dispersion of Singleâ€Walled Carbon Nanotubes and Its Application for Transparent Conductive Films. Advanced Functional Materials, 2011, 21, 2330-2337.	14.9	51

#	Article	IF	CITATIONS
91	Edge phonon state of mono- and few-layer graphene nanoribbons observed by surface and interference co-enhanced Raman spectroscopy. Physical Review B, 2010, 81, .	3.2	77
92	Efficient synthesis of graphene nanoribbons sonochemically cut from graphene sheets. Nano Research, 2010, 3, 16-22.	10.4	143
93	Bulk growth of mono- to few-layer graphene on nickel particles by chemical vapor deposition from methane. Carbon, 2010, 48, 3543-3550.	10.3	96
94	Efficient growth of high-quality graphene films on Cu foils by ambient pressure chemical vapor deposition. Applied Physics Letters, 2010, 97, .	3.3	176
95	Efficient Preparation of Large-Area Graphene Oxide Sheets for Transparent Conductive Films. ACS Nano, 2010, 4, 5245-5252.	14.6	869
96	Graphene Anchored with Co ₃ O ₄ Nanoparticles as Anode of Lithium Ion Batteries with Enhanced Reversible Capacity and Cyclic Performance. ACS Nano, 2010, 4, 3187-3194.	14.6	2,358
97	Field Emission of Single‣ayer Graphene Films Prepared by Electrophoretic Deposition. Advanced Materials, 2009, 21, 1756-1760.	21.0	624
98	Synthesis of high-quality graphene with a pre-determined number of layers. Carbon, 2009, 47, 493-499.	10.3	650
99	Metal-Catalyst-Free Growth of Single-Walled Carbon Nanotubes. Journal of the American Chemical Society, 2009, 131, 2082-2083.	13.7	258
100	Crystallographic Tailoring of Graphene by Nonmetal SiO _{<i>x</i>} Nanoparticles. Journal of the American Chemical Society, 2009, 131, 13934-13936.	13.7	68
101	Synthesis of Graphene Sheets with High Electrical Conductivity and Good Thermal Stability by Hydrogen Arc Discharge Exfoliation. ACS Nano, 2009, 3, 411-417.	14.6	807
102	Surface and Interference Coenhanced Raman Scattering of Graphene. ACS Nano, 2009, 3, 933-939.	14.6	87
103	Growth Velocity and Direct Length-Sorted Growth of Short Single-Walled Carbon Nanotubes by a Metal-Catalyst-Free Chemical Vapor Deposition Process. ACS Nano, 2009, 3, 3421-3430.	14.6	76
104	Manganese-Catalyzed Surface Growth of Single-Walled Carbon Nanotubes with High Efficiency. Journal of Physical Chemistry C, 2008, 112, 19231-19235.	3.1	37
105	Total Color Difference for Rapid and Accurate Identification of Graphene. ACS Nano, 2008, 2, 1625-1633.	14.6	135